OPERATIONAL LIMITS AND LIMITING INSTABILITIES IN TOKAMAK MACHINES

H. R. Koslowski

Forschungszentrum Jülich GmbH, Institut für Energie- und Klimaforschung 4 – Plasmaphysik
D-52425 Jülich, Germany

ABSTRACT

The optimisation of the fusion output power in a tokamak device of given size and magnetic field requires to maximise the fusion triple product $nT\tau_E$. The parameter space for safe, reliable, and stable operation of a tokamak is limited by various constraints. Operational limits of tokamak devices originate from violation of magnetohydrodynamic stability criteria or excessive radiation from impurity ions in the plasma. Exceeding the boundaries of stable operation may either result in a deterioration of plasma confinement, or even lead to the uncontrolled disruptive termination of the discharge.

I. INTRODUCTION

The need to optimise the tokamak operation in order to get a sufficient fusion yield is the main motivating force to explore and understand operational limits. As a starting point, a quite general 0-dimensional consideration of a fusion power generating machine will be presented. The thermonuclear power density (i.e. released power per volume) in a D-T plasma is

$$p_{DT} = n_D n_T \langle \sigma v \rangle \epsilon_{DT}, \qquad (1)$$

where $n_{D,T}$ are the ion densities of D and T nuclei, $\langle \sigma v \rangle$ is the rate coefficient for the fusion reaction, and $\epsilon_{DT} = 17.6\,\text{MeV}$ is the released energy per fusion reaction. The fusion power density has a maximum when the concentrations of both, D and T ions, are each 50% of the total ion density. In the temperature range between 10 keV and 20 keV the rate coefficient scales within a few % proportional to the square of the temperature, $\langle \sigma v \rangle \propto T^2$. Using the definition of the plasma beta, the ratio between kinetic plasma pressure, p, and magnetic field pressure, $\beta = 2\mu_0 p / B^2$, substituting quantities in equation 1, and integrating over the plasma volume gives

$$P_{fus} \propto p^2 V \propto \beta^2 B^4 V. \qquad (2)$$

This equation shows that the achievable fusion power of a tokamak device strongly depends on the magnetic field and the machine size, but there is a considerable dependence on the plasma pressure, i.e. the way the machine is operated. One way to increase the fusion power output of a machine is to build a larger device with a higher magnetic field. Beside the fact that especially increasing the size of the machine will increase the cost, there are technological limits. The magnetic field can not be increased arbitrarily because the required superconducting coils only allow a maximum field because superconductivity gets lost at magnetic field strengths above a critical field H_c. Another route to performance optimisation is opened due to the dependence of the fusion power on the square of the plasma pressure. Appropriate means to tailor the discharge and increase the pressure at a given magnetic field are required.

The most common operational scenario of a tokamak machine nowadays (and foreseen as base operational mode on ITER) is the so-called ELMy H-mode (*high confinement mode*). This is a plasma regime (only observed in tokamaks with a poloidal divertor) where a transport barrier at the plasma edge builds up, steepens the plasma profiles, and leads to an increase of the stored energy in the plasma [1]. The energy confinement times of H-mode plasmas have been well documented in numerous experiments on many divertor tokamaks and a scaling law based on engineering quantities has been derived [2]:

$$\tau_{E,th} \propto I_p^{0.93} B_t^{0.15} P^{-0.69} n_e^{0.41} M^{0.19} R^{1.97} \epsilon^{0.58} \kappa^{0.78} \qquad (3)$$

(I_p plasma current, B_t toroidal magnetic field, P heating power, n_e line averaged electron density, M isotope mass, R major tokamak radius, $\epsilon = a/R$ inverse aspect ratio, a minor tokamak radius, κ plasma elongation). Without going in too much detail[1], it can be seen again that increasing machine size, and increasing plasma current and density have a beneficial effect on the confinement. In addition, the plasma elongation has a strong influence on the confinement properties.

The equations above indicate which plasma parameters have to be increased in order to achieve best plasma performance in a tokamak machine of given size and magnetic field. However, there are only a few actuators for external control of plasma parameters. The density can be controlled by adjusting the gas

---

[1]For a detailed discussion of this scaling law see J. Ongena "Heating, Confinement and Extrapolation to Reactors", these proceedings.

fuelling into the plasma. The plasma current is controlled by adjusting the loop voltage through the flux change in the primary winding of the transformer. The plasma temperature can be regulated by auxiliary heating systems, e.g. neutral beam heating or wave heating in the ion cyclotron, electron cyclotron, and lower hybrid range of frequencies. As a side effect (or in some situations deliberately wanted) the plasma heating methods can drive localised currents in the plasma. This is utilised to increase plasma stability or access a certain confinement mode of the plasma.

All actions and attempts to optimise the fusion power output are constraint by operational boundaries, i.e. the plasma density can't be increased infinitely but has to be kept below the so-called density limit. The plasma current cannot be increased above a critical value without excitation of magnetohydrodynamic (MHD) instabilities. In the worst case the violation of operational limits leads to a disruption of the discharge, which is a sudden breakdown of the plasma current and a release of the stored energy to the first wall of the tokamak. The severity of operational limits can be categorised into *soft limits* which result in a deterioration of confinement and a related reduction of fusion power, and *hard limits* which eventually lead to a disruption with potentially harmful impact on the integrity of the machine.

The mechanisms leading to a deterioration of confinement or initiating a plasma disruption have to be studied in detail in order to devise strategies to avoid touching an operational limit, stabilise an instability once it occurs, or completely prevent disruptions to happen.

II. OPERATIONAL PARAMETER SPACE OF A TOKAMAK: THE HUGILL DIAGRAM

An overview on the operational space of a specific tokamak machine is usually given in form of the so-called *Hugill diagram* [3]. Figure 1 shows such a plot for the TEXTOR tokamak[2] The Hugill diagram is a plot of the inverse safety factor at the plasma surface, $1/q_a$, versus the Murakami number, $n_e R/B_t$ [4]. Because in a cylindrical approximation the edge safety factor[3] can be written as

$$q_a = 5a^2 B_t/(RI_p), \qquad (4)$$

the inverse of the edge safety factor is proportional to the plasma current I_p. Therefore the Hugill diagram

---

[2]The TEXTOR tokamak was located in the Forschungszentrum Jülich and has been in operation for 30 years until 2013. See O. Neubauer et al., *Fusion Sci. Technol.* **47** 76 (2005) for a description of the machine.

[3]The edge safety factor is infinite in a poloidal X-point divertor configuration. In those cases the safety factor q_{95} of the flux surface encompassing 95% of poloidal flux is used synonymously.
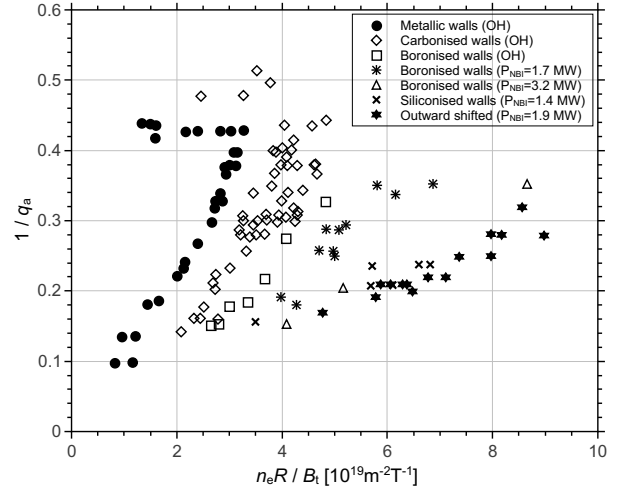

Figure 1: Hugill diagram for the TEXTOR tokamak.

can be seen as a plot of the plasma current versus the line averaged plasma density (scaled by machine size).

The operational space of the TEXTOR tokamak is shown in figure 1. The data have been collected during several years and cover various experimental campaigns with different methods of wall conditioning and ohmic as well as neutral beam injection heated scenarios [5, 6]. Careful inspection of this diagram reveals the existence of three operational boundaries.

At first one notices the absence of data points above an inverse edge safety factor of 0.5, i.e. $q_a < 2$. When the edge safety factor falls below 2 the $m = 2, n = 1$ external kink mode gets destabilised [7]. This mode grows to a large amplitude[4]. Eventually the plasma will end up in a disruption.

A second operational limit manifests itself by the absence of data points in the lower right of the diagram. For a given plasma current (which corresponds to a specific $1/q_a$ value) there exists a maximum electron density. This is an empirical boundary which is not as sharply defined as the $q_a > 2$ limit discussed before. The Hugill diagram shows that the maximum density depends on the first wall surface material of the tokamak, and on the applied heating power. Especially the improvement of wall conditioning techniques led to an increase of tokamak performance which can be attributed to cleaner plasmas with a lower effective charge, Z_{eff} [8]. There is obvious link of the achievable density with the pureness of the plasma, or in other words, the plasma can sustain a higher density when there are less impurity ions in the plasma. Impurity ions lead to an increased energy loss of the plasma which increases with density up to the critical point when the radiated power

---

[4]Mode amplitude is the radial magnetic field component, but in this context the displacement of flux surfaces is used synonymously.

equals the heating power. It can be seen in figure 1 that discharges with neutral beam heating can be stable operated at higher density.

A third limit is not very obvious but results in a lack of data points at very low density, i.e. close to the left axis of figure 1. Due to the toroidal loop voltage the electrons in the plasma experience an accelerating force. Under normal conditions the electric force is balanced by the friction force resulting from collisions. Because friction scales $\propto n_e v^{-2}$ there is a critical velocity upon which an electron is continuously accelerated and *runs away*. The Maxwellian distribution function develops a non-thermal tail. The plasma operation under these conditions has to be avoided because runaway electrons (RE) will be accelerated up to several MeV of energy and the RE beams can carry a substantial amount of energy which, when released to the first wall, may cause serious damage to the machine.

III. RADIATION LIMITS

Tokamak plasmas always contain a certain amount of impurity ions. These ions originate either from the material of the surrounding walls and are released by sputtering, or impurities are deliberately introduced in the discharge for the purpose to cool the plasma edge or divertor region in order to control plasma surface interaction. The presence of these impurity ions results in an increase of the radiation from the plasma which brings about the possibility of radiation driven instabilities.

A. Radiation Mechanisms

In a tokamak plasma different sources for radiation losses are present. The power radiated by *bremsstrahlung* due to electron-ion collisions (free-free) or recombination (free-bound) scales like

$$P_{br} \propto Z^2 \, n_e \, n_Z \, T_e^{1/2}, \tag{5}$$

where Z is the ion charge state[5], n_e and n_Z are the densities of electrons and ions in charge state Z, and T_e denotes the electron temperature. For normal tokamak operational conditions this power loss can be easily supplied by the plasma heating systems.

A more substantial power loss is due to *electron cyclotron radiation*:

$$P_c = e^4/(3\pi\epsilon_0 m_e^3 c^3) \, B^2 \, n_e \, T_e, \tag{6}$$

where e is the elementary charge, ϵ_0 the permeability of free space, m_e the electron mass, and c the velocity of light. The power radiated by electron cyclotron emission can become quite large, but it is not of concern because the plasma is optically thick at
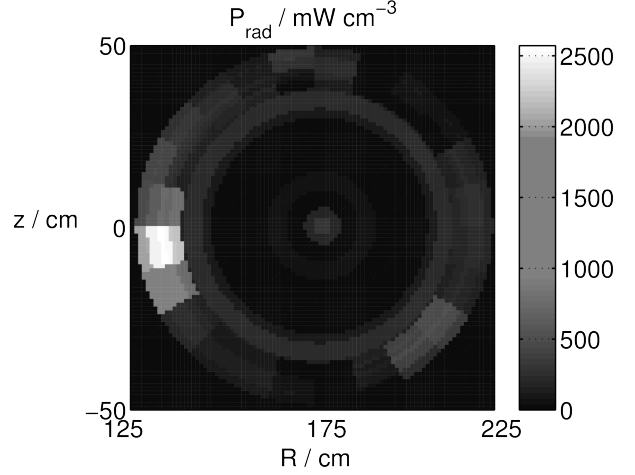

Figure 2: Asymmetric plasma radiation after onset of a MARFE in TEXTOR.

the fundamental frequency and the emitted power is immediately re-absorbed. Loss of a small fraction of radiated power can occur at the harmonic frequencies where the plasma in not optically thick.

Most important source of radiative power loss are impurity ions. They lead to an increase of bremsstrahlung losses (see equation 5) and additionally emit *line radiation* with a power density given by

$$P_R = L(T_e) \, n_e \, n_I, \tag{7}$$

where $L(T_e)$ is the cooling rate[6] [9] for a specific impurity and n_I gives the impurity density. It is important to note that the cooling rates increase when the temperature drops, i.e. $dL_{T_e}/dT_e < 0$.

B. Density Limit

The density limit in tokamaks is actually a radiation limit. When the elctron density is increased at constant pressure (i.e. without increasing the heating power), the electron temperature drops. This leads to an increase of the radiative power loss due to the above mentioned shape of the cooling rate curves. The density limit is reached when the radiative power equals the total heating power which is the sum of ohmic and auxiliary heating powers:

$$P_{rad} = P_{heat} = P_{OH} + P_{aux}. \tag{8}$$

The critical density scales like [10]

$$n_e^{crit} \propto (P_{heat}/(Z_{eff} - 1))^{1/2}. \tag{9}$$

Low effective charge and high heating power can effectively increase the density limit. This can be seen as well in the Hugill diagram figure 1 where with the progress in wall conditioning (carbonisation, boronisation) and with increased heating power larger densities were accessible.

---

[5]Due to the strong dependence on the effective charge number, the standard Z_{eff} diagnostic of a tokamak is the measurement of the visible bremsstrahlung.

[6]Other authors refer to this quantity as radiation parameter or radiation function.
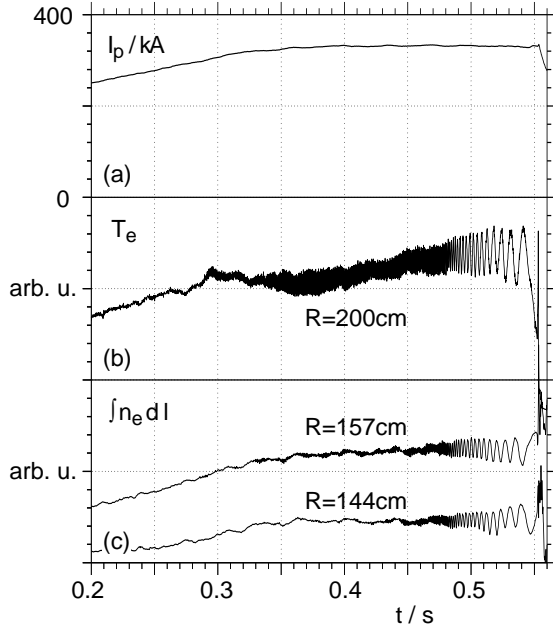
Figure 3: $m = 2, n = 1$ disruption precursor mode.

Present-day tokamaks with metal walls and/or state-of the art wall cleaning methods and sufficient heating power installed would allow for a rather high density limit. Unfortunately, it turns out that the radiative density limit is not dominated by a symmetric radiation belt following equation 9 but is determined by a variety of other mechanisms [11]. Particle transport at the edge, plasma detachment and recycling phenomena whith plasma cooling being a key element of them all start to play a role. One important and rather common phenomenon in this context is the appearance of the so-called MARFE[7] [12]. In a situation with local plasma cooling the characteristic shape of the cooling rate curves leads to a self amplifying *condensation* process most often resulting in a radiation collapse. The requirement of pressure balance results in a local, cold and very dense plasma, the MARFE. Figure 2 shows a tomographic reconstruction of the poloidal radiation distribution during a MARFE. The appearance of the MARFE is strongly correlated with the recycling flux from the plasma edge [13]. Reducing this particle flux by moving the plasma away from the surrounding walls allows for higher densities (see points labelled *outward shifted* in figure 1). The data from many tokamaks has been analysed in detail [11] and a surprisingly simple scaling law could be derived:

$$\overline{n}_{e,G} = \kappa \overline{j}, \qquad (10)$$

with $n_{e,G}$ the maximum line-averaged density in units of $10^{20}\,\mathrm{m}^{-3}$, κ the elongation of the poloidal plasma cross section, and $\overline{j}$ the poloidal average of the current density in units of MAm^{-2}. Despite it's simplicity

this simple formula has been found to well approximate the density limit in a variety of tokamaks of different size.

C. Impurity Accumulation

Nowadays tokamak are more and more equipped with limiters and divertor tiles made of high-Z materials like tungsten due to their high melting temperatures and low sputtering rates. When off-normal events lead to increased thermal and particle loads high-Z material may be eroded and released to the plasma where it is transported toward the plasma centre. The strong radiation causes local cooling and flat or even hollow temperature profiles. Because the electrical conductivity scales $\sigma \propto f(Z_{eff})T_e^{3/2}$ with temperature a decreases of the central plasma current follows and enforces the temperature decay and further accumulation of the high-Z impurity on plasma axis.

IV. BETA LIMIT

In the introduction it has been shown that the increase of beta

$$\beta_t = 2\mu_0 \langle p \rangle / B_t^2, \qquad (11)$$

where $\langle p \rangle$ is the volume averaged plasma pressure, is a rational way to increase fusion performance and make best use of the applied toroidal magnetic field B_t. This gives rise to the question, how large the plasma pressure can get before MHD instabilities become destabilised.

A. The Ideal Beta Limit

The maximum plasma pressure which can be confined by a given magnetic field has been calculated by Troyon [14]. In his calculations he considered stability against (i) the Mercier criterion [15], (ii) ballooning modes, and (iii) the $n = 1$ free-boundary kink mode. It has been found that the latter determines the upper limit on beta. For circular plasma cross section a simple scaling law for the poloidal beta[8] has been found:

$$\beta_p^{max} = 0.14\,(R/a)\,q_a. \qquad (12)$$

More general, the maximim beta β_m for a given configuration[9] can be written as

$$\beta_m = g\frac{I}{aB_t} \qquad (13)$$

where g is named the *Troyon factor* and a value of $g = 2.8$ the Troyon limit. The quantity

$$\beta_N = \frac{\beta}{I/(aBt)} \qquad (14)$$

---

[7]The acronym MARFE stands for *Multifacetted Asymmetric Radiation From the Edge*.

[8]Same as toroidal beta in equation 11 but toroidal field is replaced by poloidal field B_p.

[9]Here configuration means plasma shape.

is called normalised beta. The stability limit can then be simply expressed as $\beta_N < g$. It turns out that the Troyon factor depends on the shape of the current density profile and can be approximated in many cases by $g = 4l_i$, where i_i is the internal inductance of the plasma.

B. Resistive Wall Modes

A certain operation mode of tokamaks, the so-called advanced scenario, makes use of an elevated q-profile, a broad current density distribution, and steep pressure gradients which lead to a large bootstrap current fraction. In this scenario the external kink mode plays the limiting role. The mode can be stabilised by a close fitting conducting wall. This will result in a somewhat higher maximum beta value. Due to the conducting wall the growth rate of the external kink is reduced to the inverse of the resistive time constant of the wall. Depending on the properties of the stabilising wall, the achievable beta is in the range

$$\beta^{no-wall} < \beta < \beta^{ideal-wall}. \tag{15}$$

In this context the beta limit is called the *resistive wall mode* (RWM) limit. Stabilisation of the RWM is proposed via two different mechanisms: (i) dissipation of the free energy of the mode by fast plasma rotation, and (ii) active feedback control to cancel the RWM field by a set of saddle coils mounted inside the vacuum vessel [16].

C. (Neoclassical) Tearing Modes[10]

In contrast to kink modes which are driven by the plasma pressure, a class of modes named *tearing modes* are driven by the radial gradient of the plasma current. These modes, when destabilised, form so-called magnetic islands which are radially and poloidally localised regions where reconnection of magnetic field lines occurs and the magnetic topology is changed. The growth of tearing modes depends on the tearing parameter Δ' defined as

$$\Delta'(w) = \frac{1}{B_r} \left. \frac{\partial B_r}{\partial r} \right|_{r_s+w/2}^{r_s-w/2}, \tag{16}$$

where w is the island width and r_s the radius of the rational surface where the mode grows [17]. A positive Δ' will destabilise the mode. The growth rate depends on the resistivity η of the plasma and is approximately given by

$$\frac{dw}{dt} \simeq \frac{\eta}{2\mu_0} \Delta'(w). \tag{17}$$

Tearing modes can grow to rather large size with a radial width of 10%-20% of the minor plasma radius.

An example of a tearing mode is shown in figure 3. Here the plasma current (a), the electron temperature at about half radius (b), and two interferometer chords (c) are shown. The time traces of T_e and n_e measurements show a characteristic modulation which results from the flattening of the plasma profiles across the island[11] and the diamagnetic drift motion. It can be seen in the figure that the island rotation frequency slows down when the island size gets larger.

A common observation in almost all tokamaks is that the ideal beta limit can only be reached transiently but that the stationary achievable beta values are lower [18]. This behaviour has been found to be caused by the onset of a $m = 3, n = 2$ or $m = 2, n = 1$ tearing modes. Strangely, the Δ' parameter of these modes is negative, i.e. the modes should be stable. These modes have been named *neoclassical tearing modes* (NTM) and their growth can be described by a generalised Rutherford equation [18]. Additional to the tearing parameter this equation contains two pressure driven contributions. One term is destabilising and originates from the loss of bootstrap current due to the pressure profile flattening in the island. The second term is assumed to be stabilising and results from a polarisation current within the island. Neoclassical tearing modes are usually a soft limitation, i.e. the discharge does not disrupt but the confinement gets deteriorated. Plasma disruptions are possible in case the $m = 2, n = 1$ neoclassical tearing mode gets unstable. A widely investigated method for stabilisation of NTMs is to replace the missing bootstrap current in the island by non-inductively driven current using ECRH wave injection or lower hybrid current drive[12] [19, 20].

V. THE CURRENT LIMIT

The q_a-limit

$$q_a > 2 \tag{18}$$

has been already mentioned when discussing the Hugill diagram (figure 1). This is an hard limitation and falling below this value will unavoidably end up with a disruption. Because the density increases with plasma current, increasing the current is an easy way to achieve better confinement, as can be seen by the proportionality of the energy confinement time with plasma current (see equation 3). The main implication of the q_a-limit is that there is a maximum sustainable plasma current at a given toroidal magnetic field. But even at q_a values above 2 but close to 2 the plasma may be already affected by MHD stability issues due to the growth of the $m = 2, n = 1$ tearing

---

[10]This section is just for completeness and kept rather concise, a much more detailed article by H. R. Wilson on "Neoclassical Tearing Modes" can be found elsewhere in these proceedings.

[11]Magnetic islands are commonly referred as O-points of the mode, whereas the crossing of the island separatrix between O-points is labelled the X-point.

[12]See E. Westerhof's article on "Non-inductive Current Drive" in these proceedings.
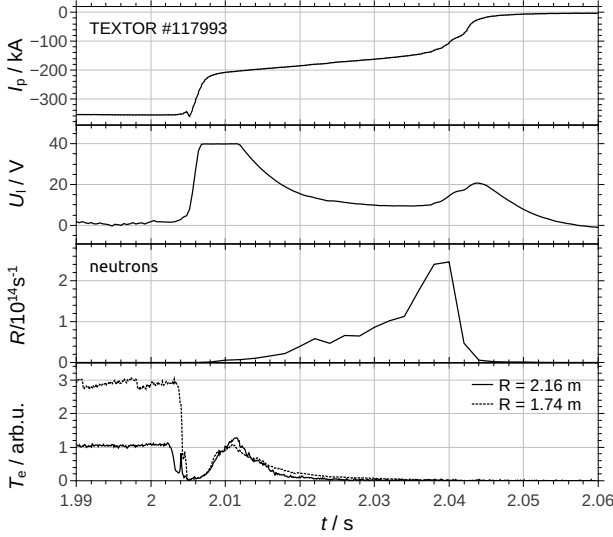
Figure 4: Plasma disruption with runaway electron plateau. Traces from top to bottom are (i) plasma current, (ii) loop voltage (maesurement is saturated), (iii) neutron rate, and (iv) electron temperature (centre and edge).

mode. There is no simple criterion to decide whether this mode is unstable because the shape of the current density profile, the plasma pressure, plasma rotation, and the proximity to a conducting wall influence the stability. As a rule of thumb one can say that the excitation of the $m = 2, n = 1$ mode becomes more likely at lower edge safety factor q_a. Most plasma scenarios today use values of 3 or larger.

VI. LOCKED MODES AND ERROR FIELDS

An MHD perturbation like a kink or tearing modes are usually frozen in the plasma fluid according to Alfvén's theorem. As a consequence modes rotate due to drifts or momentum input by neutral particle injection. A growing mode in the plasma will experience friction caused by induced eddy currents in the wall and slow down the plasma rotation. Eventually the mode can lock to the wall and the rotation in the tokamak frame stands still. The growths rate of the mode after locking is determined by the resistivity of the tokamak first wall and much larger than in the rotating state. In many cases mode locking is observed to be a precursor to a disruptions. The slowing down and locking leading to fast mode growth and disruption can be seen in figure 3. Here a disruption starts at $t = 0.552\,\mathrm{s}$ shortly after the mode stopped and a fast growths (see T_e signal) set in.

A common source for the excitation of locked modes are intrinsic error fields. These fields can arise from small alignment errors of the coils systems. Already low error field amplitudes of the order

$B_r/B_t \approx 10^{-4}$ (B_r is the radial component of the error field) have been found sufficient to excite locked $n = 1$ modes. An error field of this size is expected on ITER due to small coil misalignments [21].

The critical mode amplitude for mode excitation has been investigated in a variety of tokamaks and a power law scaling expression has been derived [22]:

$$B_r/B_t \propto n_e^{\alpha_n} B_t^{\alpha_B} q_{95}^{\alpha_q} R^{\alpha_R}. \qquad (19)$$

The exponents α_x show a rather large scatter between individual machines, good agreement has been found only for α_n which is about 1, i.e. the resistance against error field driven modes increases linearly with plasma density. α_B is always negative, meaning that acceptable error field levels become even smaller at larger machines.

Plasma rotation generally increases the threshold for mode excitation. Momentum input which adds to the diamagnetic drift will act stabilising, but when the fluid rotation is compensated by external momentum input the error field threshold shows a minimum [23].

VII. VERTICAL STABILITY

A circular shaped plasma is stable with respect to vertical displacements if the field index

$$n = -\frac{R}{B_v}\frac{\mathrm{d}B_v}{\mathrm{d}R} \qquad (20)$$

is larger than zero [7]. However, vertical elongation κ has a positive effect on the confinement (see equation 3) and most of the tokamaks are operated with elongated plasma shape. A drawback is that the plasma column becomes unstable with respect to vertical displacements. The growth rate of this vertical displacement event (VDE) depends on plasma elongation and can become rather large. A loss of control will results in the plasma either touching on the divertor or armour tiles at the top. Large heat loads and halo currents[13] arise before the plasma current eventually disrupts. The growth rate of the VDE can be decreased down by a close fitting conducting wall (similar to RWM stabilisation). Experiments on the Swiss tokamak TCV have shown that growth rates of several $1000\,\mathrm{s}^{-1}$ could be feedback stabilised [24].

VIII. DISRUPTIONS

A disruption is a fast decay of the plasma current as a consequence of a severe plasma instability, an operational limit, or a loss of plasma control. The evolution of a disruption can be divided into several stages

---

[13]Halo currents arise when the plasma column touches the wall and a fraction of the plasma current flows partly in the wall.

[10]. An initiating event causes an unstable state, often accompanied by changes of the current density distribution. Precursor like mode oscillations appear next before the actual disruption starts. There are two distinct phases: (i) the thermal quench (TQ) during which the temperature profile collapses and the stored plasma energy is released to the surrounding walls, and (ii) the current quench (CQ) during which the plasma current decays very fast and the magnetic energy is released. Energetic electrons with energies up to several MeV can be generated during the CQ because the tokamak loop voltage rises due to Lenz's law.

Disruptions pose a threat to the integrity of a tokamak because they could result in (i) radiative and convective heat loads on plasma facing components which may cause melting or evaporation, (ii) strong $j \times B$ forces on the vacuum vessel due to induced eddy currents and halo currents, and (iii) a beam of high energetic electrons which can carry a significant fraction of the plasma current and may cause severe damage when hitting plasma facing components.

Disruption studies are at high urgency for ITER [21] and methods for reliable early detection, avoidance, and mitigation need to be developed.

A. Runaway Electrons

Runaway electrons (RE) are generated when the friction force due to collisions gets smaller than the electric force due to the toroidal loop voltage. A relativistic calculation of the critical electric field required for electrons to run away yields

$$ E_{crit} = \frac{n_e e^3 \ln\Lambda}{4\pi\epsilon_0^2 m_e c^2} \qquad (21) $$

where $\ln\Lambda$ is the Coulomb logarithm, e and m_e charge and mass of an electron, and c the speed of light. For normal tokamak conditions the electric field is less than the critical electric field, so no runaway electrons are generated. At very low density the loop voltage is large enough to produce runaway electrons. These conditions are at the left edge of the Hugill diagram (figure 1). Although in a strict sense the generation of runaway electrons is no operational limit, tokamak operation at those conditions is usually avoided because of the potential damage they may cause.

Once there is a population of energetic electrons an avalanche-like process due to small angle collisions with thermal electrons sets in [25]. This secondary generation process will be dominant on large tokamaks.

B. Disruption Avoidance

The optimum approach to solve the disruption problem would be to avoid any disruption happening. This requires a reliable way to detect the very early stage of a disruption, e.g. a precursor, and some

actuators to rectify whatever went wrong and to regain plasma control. The application of neural networks for early detection of disruptions is under investigation and shows good progress [26]. For certain classes of disruptions a direct detection of a precursor mode and the use of neutral beam injection in order to enhance plasma rotation and stabilise the mode has proven to be successful [27].

C. Disruption Mitigation

The situation that a disruption cannot be avoided may arise. In this case a way to deliberately shut down the plasma discharge and to ameliorate the consequences of a disruption is required. The shutdown procedure has to be designed in a way which keeps $j \times B$ forces on vessel and coil systems within acceptable limits, dissipates the plasma stored thermal and magnetic energies in a way which does not lead to localised overheating of plasma facing components, and prevents that a part of the plasma current is transformed into REs. The energy balance for a shutdown prcedure is as follows:

$$ W_{th} + W_{mag} = W_{rad} + W_{coupled} + W_{conv} \; (+W_{RE}) \qquad (22) $$

The thermal plasma energy W_{th} and the magnetic energy W_{mag} are converted in to radiated energy W_{rad} (this is preferred because radiation is distributed on a large wall surface), the energy $W_{coupled}$ which is coupled via the mutual inductances into the tokamak coil systems, the part of the energy which is convected by plasma wall contact W_{conv}, and the energy which is carried by RE electrons. Especially the latter two components result in small wetted areas and large local heat loads. Various disruption mitigation methods have been proposed: (i) A fast controlled ramp-down of the plasma current seems to be a good solution but is not always possible. It needs a rather large warning time, and the plasma density (and radiation) may not decrease with the required rate thus provoking a density limit disruption. (ii) Injection of so-called *killer pellets*[14] or *shattered pellets*[15] in order to force the plasma into a radiation limit disruption. (iii) *Massive gas injection* [28] using specially designed fast valves is another promising method to deliberately induce a radiation collapse. This method is presently under investigation on many tokamaks.

IX. SUMMARY

The operational limits of a tokamak machine arise from a variety of different physical mechanisms. The density limit is actually defined by the balance between plasma radiation and heating power. Clean

---

[14]Similar to frozen hydrogen fuelling pellets but made of neon or argon.

[15]Nobel gas pellets of large size which are shot against a solid target which disaggregates the pellet before entry into the plasma.

plasmas and good wall conditioning together with sufficient heating power can assure stable operation close to this limit. A limitation on the maximum plasma current at a given toroidal field results from the MHD stability properties of the $m = 2, n = 1$ mode. The generation of runaway electrons constrains the operation at low density. The ideal beta limit originates from pressure driven $n = 1$ kink instabilities. More of importance is the so-called *practical beta limit* which is due to the neoclassical tearing mode and is the most frequent limitation to plasma performance. Disruptions can cause damage to the machine pose the most severe problem on large tokamaks requiring an adequate mitigation method.

REFERENCES

1. F. Wagner et al., "Regime of Improved Confinement and High Beta in Neutral-Beam-Heated Divertor Discharges of the ASDEX Tokamak", *Phys. Rev. Lett.*, **49**, 1408 (1982).

2. ITER Physics Expert Groups on Confinement and Transport and Confinement Modelling and Database, "Chapter 2: Plasma confinement and transport", *Nucl. Fusion*, **39**, 2175-2249 (1999).

3. S. J. Fielding et al., "High-Density Discharges with Gettered Torus Walls in DITE", *Nucl. Fusion* **17** 1382 (1977).

4. M. Murakami et al., "Some Observations on Maximum Densities in Tokamak Experiments", *Nucl. Fusion* **16** 347 (1976).

5. G. Waidmann et al., "Density Limits and Evolution of Disruptions in Ohmic TEXTOR Plasmas", *Nucl. Fusion*, **32**, 645 (1992).

6. J. Rapp et al., "Scaling of Density Limits with Respect to Global and Edge Parameters in TEXTOR-94", in Proc. 26th EPS Conf. on Contr. Fusion and Plasma Physics, Maastricht, *ECA* **23J**, 665 (1999).

7. J. A. Wesson, "Hydrodynamic Stability of Tokamaks", *Nucl. Fusion*, **18**, 87 (1978).

8. J. Winter, "Wall conditioning in fusion devices and its influence on plasma performance", *Plasma Phys. Control. Fusion*, **38**, 1503 (1999).

9. D. E. Post et al., "Steady-state radiative cooling rates for low-density high-temperature plasmas", *At. Data Nucl. Data Tables*, **20**, 397 (1977).

10. F. C. Schüller, "Disruptions in Tokamaks", *Plasma Phys. Control. Fusion*, **37**, A135 (1995).

11. M. Greenwald, "Density Limits in Toroidal Plasmas", *Plasma Phys. Control. Fusion*, **44**, R27 (2002).

12. B. Lipschultz, "Review of MARFE Phenomena in Tokamaks", *J. Nucl. Mater.*, **145-147**, 15 (1987).

13. P. C. de Vries et al., "Influence of Recycling on the Density Limit in TEXTOR-94", *Phys. Rev. Lett.* **80**, 3519 (1998).

14. F. Troyon et al., "MHD-Limits to Plasma Confinement", *Plasma Phys. Control. Fusion*, **26**, 209 (1984).

15. C. Mercier, "A necessary condition for hydromagnetic stability of plasma with axial symmetry", *Nucl. Fusion* **1** 47 (1960).

16. M. S. Chu and M. Okabayashi, "Stabilisation of the external kink and the resistive wall mode", *Plasma Phys. Control. Fusion*, **52**, 123001 (2010).

17. H. P. Furth et al., "Tearing mode in the cylindrical tokamak" *Phys. Fluids*, **16**, 1054 (1973).

18. O. Sauter et al., "Beta Limits in Long-Pulse Tokamak Discharges", *Phys. Plasmas*, **4**, 1654 (1997).

19. H. Zohm et al., "Experiments on Neoclassical Tearing Mode Stabilisation by ECCD in ASDEX-Upgrade", *Nucl. Fusion*, **39**, 577 (1999).

20. C. D. Warrick et al., "Complete Stabilisation of Neoclassical Tearing Modes with Lower Hybrid Current Drive on COMPASS-D", *Phys. Rev. Lett.*, **85**, 574 (2000).

21. T. Hender et al., "MHD Stability, Operational Limits and Disruptions" (Chapter 3 in "Progress in the ITER Physics Base"), *Nucl. Fusion*, **47**, S128 (2007).

22. R. J. Buttery et al., "Error field mode studies on JET, COMPASS-D and DIII-D, and implications for ITER", *Nucl. Fusion*, **39**, 1827 (1999).

23. H. R. Koslowski et al., "Dependence of the Threshold for Perturbation Field Generated m/n = 2/1 Tearing Modes on the Plasma Fluid Rotation", *Nucl. Fusion*, **46**, L1 (2006).

24. F. Hofmann et al., "Vertical Position Control in TCV: Comparison of Model Predictions with Experimental Results", *Nucl. Fusion*, **40**, 767 (2000).

25. R. Jaspers et al., "Disruption Generated Runaway Electrons in TEXTOR and ITER", *Nucl. Fusion*, **36**, 367 (1996).

26. G. Pautasso et al., "Prediction and mitigation of disruptions in ASDEX Upgrade", *J. Nucl. Mater.*, **290-293**, 1045 (2001).

27. A. Krämer-Flecken et al., "Heterodyne ECE Diagnostic in the Mode Detection and Disruption Avoidance at TEXTOR", *Nucl. Fusion*, **43**, 1437 (2003).

28. D. G. Whyte et al., "Disruption mitigation with high-pressure noble gas injection", *J. Nucl. Mater.*, **313-316**, 1239 (2003).